



RESEARCH LETTER

10.1029/2022GL098720

Mixed Layer Depth Promotes Trophic Amplification on a Seasonal Scale

Tianfei Xue¹ , Ivy Frenger¹ , Andreas Oschlies¹ , Charles A. Stock² , Wolfgang Koeve¹ , Jasmin G. John^{2,3} , and A. E. Friederike Prowe¹ ¹GEOMAR Helmholtz Centre for Ocean Research Kiel, Kiel, Germany, ²NOAA Geophysical Fluid Dynamics Laboratory, Princeton University, Princeton, NJ, USA, ³NOAA/OAR/Atlantic Oceanographic and Meteorological Laboratory, Miami, FL, USA

Key Points:

- Environmental factors strongly affect plankton trophodynamics on a seasonal scale
- Seasonal trophic amplification in the Humboldt system is driven by mixed layer dynamics
- Mixed layer depth and food chain efficiency correlate also in other productive regions

Supporting Information:

Supporting Information may be found in the online version of this article.

Correspondence to:

T. Xue,
txue@geomar.de

Citation:

Xue, T., Frenger, I., Oschlies, A., Stock, C. A., Koeve, W., John, J. G., & Prowe, A. E. F. (2022). Mixed layer depth promotes trophic amplification on a seasonal scale. *Geophysical Research Letters*, 49, e2022GL098720. <https://doi.org/10.1029/2022GL098720>

Received 21 MAR 2022

Accepted 7 JUN 2022

Author Contributions:

Conceptualization: Tianfei Xue, Ivy Frenger, Andreas Oschlies, Charles A. Stock, A. E. Friederike Prowe**Formal analysis:** Tianfei Xue**Methodology:** Tianfei Xue, A. E. Friederike Prowe**Project Administration:** Ivy Frenger, Andreas Oschlies**Supervision:** Ivy Frenger, Andreas Oschlies, A. E. Friederike Prowe**Writing – original draft:** Tianfei Xue**Writing – review & editing:** Tianfei Xue, Ivy Frenger, Andreas Oschlies, Charles A. Stock, Wolfgang Koeve, Jasmin G. John, A. E. Friederike Prowe

Abstract The Humboldt Upwelling System is of global interest due to its importance to fisheries, though the origin of its high productivity remains elusive. In regional physical-biogeochemical model simulations, the seasonal amplitude of mesozooplankton net production exceeds that of phytoplankton, indicating “seasonal trophic amplification.” An analytical approach identifies amplification to be driven by a seasonally varying trophic transfer efficiency due to mixed layer variations. The latter alters the vertical distribution of phytoplankton and thus the zooplankton and phytoplankton encounters, with lower encounters occurring in a deeper mixed layer where phytoplankton are diluted. In global model simulations, mixed layer depth appears to affect trophic transfer similarly in other productive regions. Our results highlight the importance of mixed layer depth for trophodynamics on a seasonal scale with potential significant implications, given mixed layer depth changes projected under climate change.

Plain Language Summary The Humboldt Upwelling System is a fishery-important region. A common assumption is that a certain amount of phytoplankton supports a proportional amount of fish. However, we find that a small seasonal change in phytoplankton can trigger a larger variation in zooplankton. This implies that one may underestimate changes in fish solely based on phytoplankton. Using ecosystem model simulations, we investigate why changes of phytoplankton are not proportionally reflected in zooplankton. The portion of phytoplankton that ends up in zooplankton is controlled by the changing depth of the surface ocean “mixed layer.” The “mixed layer” traps both the phytoplankton and zooplankton in a limited amount of space. When the “mixed layer” is shallow, zooplankton can feed more efficiently on phytoplankton as both are compressed in a comparatively smaller space. We conclude that in the Humboldt System, and other “food-rich” regions, feeding efficiently, determined by the “mixed layer,” is more important than how much food is available.

1. Introduction

The Humboldt Upwelling System is one of the most important regions contributing to global fisheries, though the origin of the high fish production relative to phytoplankton production remains unclear. Benefiting from constantly upwelled nutrients, the Humboldt system is highly productive throughout the year, supporting a productive zooplankton community and further nourishing a rich small pelagic fish stock (e.g., anchovies and sardines; Bakun & Weeks, 2008). While Pauly and Christensen (1995) suggest that 25% of phytoplankton production is required to sustain fish catch in upwelling regions, Friedland et al. (2012) found phytoplankton production to be a poor predictor for fishing yield. Phytoplankton and fish production are related by trophodynamics which may boost or buffer responses of different trophic levels to changes in environmental conditions. The terms “trophic amplification” and “trophic attenuation,” therefore, were introduced to describe a change in a higher trophic level that is more or less prominent than in a lower trophic level, respectively (Kirby & Beaugrand, 2009).

Traditional theory (Lindeman, 1942) assumes that the portion of phytoplankton production transferred to fish (food chain efficiency) depends on the efficiency of energy transfer across trophic levels (trophic transfer efficiency) and the length of the food chain (food chain length). Different biomes strongly differ in their trophic transfer efficiencies and food chain lengths (Pauly & Christensen, 1995; Ryther, 1969). For these differences, multiple factors play a role, such as physical-biogeochemical conditions (e.g., temperature, light and nutrients; Du Pontavice et al., 2020; Dickman et al., 2008) and multiple ecological processes (e.g., zooplankton feeding

© 2022 The Authors.

This is an open access article under the terms of the [Creative Commons Attribution-NonCommercial License](#), which permits use, distribution and reproduction in any medium, provided the original work is properly cited and is not used for commercial purposes.

strategy; Heneghan et al., 2016; Mitra et al., 2014; Prowe et al., 2019). Previous model studies resolving ecology up to mesozooplankton suggest that trophic transfer efficiency is affected by hydrodynamically driven predator-prey encounter (Legendre & Rassoulzadegan, 1996) and growth efficiencies of each trophic level, while food chain length is determined, amongst others, by phytoplankton composition (Stock et al., 2014).

The Humboldt system is characterized by a strikingly high food chain efficiency, even compared to other eastern boundary upwelling systems (Chavez et al., 2008). The lower trophic ecosystem is highly seasonal with plankton, and export efficiency, oddly opposing the seasonality of upwelling of nutrient-rich waters (Echevin et al., 2008; Xue et al., 2022). The seasonality of lower trophic levels due to environmental conditions is expected to affect higher trophic levels in the Humboldt system. To better understand the Humboldt system trophodynamics, we derive equations for trophic transfer efficiency and food chain length based on Ulanowicz (1995). It allows us to disentangle their roles in variations of the food chain efficiency and identify a dominant contribution of trophic transfer efficiency. The mechanism is regulation of predator-prey encounters due to compression and dilution of prey with varying mixed layer depths. We then extrapolate our findings to the global scale by using the seasonal cycle of observational estimates and simulations from two global models to investigate how the governing mechanism may act in other biomes that are similarly productive as the Humboldt system.

2. Methods

2.1. Regional Physical - Biogeochemical Model: CROCO-BioEBUS

We use a three-dimensional regional physical model CROCO (Coastal and Regional Ocean COmmunity model; Shchepetkin & McWilliams, 2005) coupled with the biogeochemical model BioEBUS (Biogeochemical model for the Eastern Boundary Upwelling Systems; Gutknecht et al., 2013) for analyses of the seasonality of trophodynamics. A detailed description of the model set-up and evaluation can be found in Xue et al. (2022). We focus on the 200 km wide band off the Peruvian coast (Figure S1b in Supporting Information S1) characterized by high phytoplankton production that overlaps with the coastal habitat of anchovy (Bertrand et al., 2004).

CROCO is a free-surface, split-explicit regional ocean circulation model. We employ a two-way nesting approach and use the embedded “small” domain for analyses. It has a resolution of $1/12^\circ$ extending from 5°N to 31°S and 69°W to 102°W , and 32 vertical sigma levels, with a finer resolution toward the surface of 0.5–2 m in shallow waters. Initial and boundary conditions and surface forcing are provided by monthly climatological SODA reanalysis from 1990 to 2010 (Carton & Giese, 2008) and COADS heat and freshwater flux data (Worley et al., 2005). BioEBUS is a nitrogen-based model with four plankton groups representing small and large phytoplankton along with microzooplankton and mesozooplankton (Gutknecht et al., 2013). Microzooplankton graze on both phytoplankton with a preference for small phytoplankton, while mesozooplankton graze on the other three groups, favoring microzooplankton the most and small phytoplankton the least. Initial and boundary conditions for phytoplankton are based on monthly climatological SeaWiFS (O’Reilly et al., 1998), nitrate and oxygen concentrations are taken from CARS (Ridgway et al., 2002). The model is climatologically forced for 30 years and the last 5 years are used for analyses.

2.2. Analytical Derivation of Trophic Transfer Efficiency and Food Chain Length

Following the original concept in Kirby and Beaugrand (2009), we define “seasonal trophic amplification” as a more prominent relative seasonal amplitude of higher trophic level (mesozooplankton) net production compared to that of a lower trophic level (phytoplankton). To investigate the disproportionate energy transfer, we attribute variations of food chain efficiency (FCE) to variations of trophic transfer efficiency (TTE) and food chain length (FCL). We calculate TTE and FCL based on the amount of energy transferred between trophic levels (TL), applying the analytical formulations in Ulanowicz (1995). This approach accounts for the fact that food webs typically represent “webs” where predators graze on multiple prey types and converts them into “chains.” In our derivations below we calculate net production (NP, in mmol N m^{-3}) of each plankton group as the part that is potentially available for the next trophic level: Net phytoplankton production (NP_{sphy} and NP_{lphy} of small and large phytoplankton, respectively) is computed as the nitrogen uptake subtracting exudation; net zooplankton production (NP_{szoo} and NP_{lzoo} of micro- and mesozooplankton, respectively) is the assimilated fraction of grazing (grazing minus fecal pellets) minus respiration.

2.2.1. Food Chain Length

We define FCL as the highest trophic position, mesozooplankton in our model. Following Ulanowicz (1995), we define a trophic transformation matrix \mathbf{T} (Equation 1) that allows the mapping of net production of the plankton compartments of the model food web to a chain. The rows of \mathbf{T} represent trophic levels, and the columns are different plankton groups, that is, small and large phytoplankton and then small and large zooplankton.

$$\mathbf{T} = \begin{pmatrix} 1 & 1 & 0 & 0 \\ 0 & 0 & 1 & D_{pz} \\ 0 & 0 & 0 & D_{zz} \\ 0 & 0 & 0 & 0 \end{pmatrix} \quad (1)$$

$$\text{with } D_{pz} = \frac{G_{lzo0}^{sphy} + G_{lzo0}^{lphy}}{G_{lzo0}}, \text{ and } D_{zz} = \frac{G_{lzo0}^{szoo}}{G_{lzo0}},$$

$G_{lzo0} = G_{lzo0}^{sphy} + G_{lzo0}^{lphy} + G_{lzo0}^{szoo}$ represents total mesozooplankton grazing. D_{pz} and D_{zz} are the fractions of phyto- and microzooplankton in the mesozooplankton diet. By definition, the sums of the columns add up to 1, that is $D_{pz} + D_{zz} = 1$. Mesozooplankton (column 4) can be considered partially trophic level 2 (TL₂, row 2) and 3 (TL₃, row 3) as it grazes on both phytoplankton (TL₁, row 1) and microzooplankton (TL₂, row 2). The trophic level of mesozooplankton, that is FCL, can then be calculated as:

$$\text{FCL} = \text{TL}_{lzo0} = 2 * D_{pz} + 3 * D_{zz} = 2 * (D_{pz} + D_{zz}) + D_{zz} = 2 + D_{zz} \quad (2)$$

Hence, a value of two indicates complete herbivory, 2.5 50% herbivory, 50% carnivory, and 3 complete carnivory.

2.2.2. Trophic Transfer Efficiency

We calculate TTE based on the net production of the plankton compartments combined with the trophic transformation matrix. First, we get the net production for each trophic level (NP_{TL}) by multiplying the trophic transformation matrix \mathbf{T} with the vector composed of the net production values of each plankton compartment:

$$\begin{pmatrix} \text{NP}_{\text{TL}_1} \\ \text{NP}_{\text{TL}_2} \\ \text{NP}_{\text{TL}_3} \\ \text{NP}_{\text{TL}_4} \end{pmatrix} = \mathbf{T} * \begin{pmatrix} \text{NP}_{\text{sphy}} \\ \text{NP}_{\text{lphy}} \\ \text{NP}_{\text{szoo}} \\ \text{NP}_{\text{lzo0}} \end{pmatrix} \quad (3)$$

Thus, net production of TL₃ refers to the part of mesozooplankton that is grazing on microzooplankton

$$\text{NP}_{\text{TL}_3} = D_{zz} * \text{NP}_{\text{lzo0}} \quad (4)$$

Then, we define TTE as the ratio of net production between trophic levels (TL):

$$\text{TTE}_n = \frac{\text{NP}_{\text{TL}_{n+1}}}{\text{NP}_{\text{TL}_n}} \quad (5)$$

2.2.3. Food Chain Efficiency

Based on the FCL (Section 2.2.1) and the TTE (Section 2.2.2), we obtain an equation for the FCE. Equation 5 allows us to express NP_{TL₃} in terms of the production of lowest trophic level and the subsequent energy transfers to TL₃:

$$\text{NP}_{\text{TL}_3} = \text{NP}_{\text{TL}_2} * \text{TTE}_2 = (\text{NP}_{\text{TL}_1} * \text{TTE}_1) * \text{TTE}_2 \quad (6)$$

Equating Equations 4 and 6 and considering Equation 2 leads to an equation relating mesozooplankton net production (NP_{zoo}) with net phytoplankton production (NP_{phy}), TTE and FCL:

$$NP_{\text{zoo}} = NP_{\text{phy}} \frac{TTE_1 \cdot TTE_2}{FCL - 2} \quad (7)$$

From this follows that FCE, here representing the ratio of net mesozooplankton production to phytoplankton production, is directly linked with TTE and anti-correlated with FCL:

$$FCE = \frac{NP_{\text{zoo}}}{NP_{\text{phy}}} = \frac{TTE_1 \cdot TTE_2}{FCL - 2} \quad (8)$$

2.2.4. Predator-Prey Encounter Efficiency (EE)

To assess the importance of predator-prey vertical encounter efficiency for TTE, we define EE within the water column as:

$$EE = \frac{\sum_{i=1}^n (\text{prey}_i \cdot \text{pred}_i)}{\sum_{i=1}^n \text{prey}_i \cdot \sum_{i=1}^n \text{pred}_i} \quad (9)$$

n stands for the number of vertical grid boxes. prey_i and pred_i represent the biomass concentrations of predator and prey within the grid box i . EE is calculated by weighting the thicknesses of the grid boxes. It is affected by both vertical distributions and biomass concentration of predator and prey, with the value ranging from 0 to 1. An EE of 0 means no overlap between predator and prey. A value of 1 means both predator and prey are concentrated in the same single grid box, reaching the full potential of predator-prey trophic transfer (every predator can eat all prey).

2.3. Global Models and Observation

To test the global applicability of our findings in the Humboldt system, we use two contrasting global models: (a) the University of Victoria Earth System Climate Model version 2.9 (UVic-model; Weaver et al., 2001; Keller et al., 2012) with relatively coarse resolution and simple food web structure; (b) the Geophysical Fluid Dynamics Laboratory Earth System Model 2.6 (GFDL-model; Stock et al., 2017) with relatively fine resolution and complex food web structure.

The UVic-model uses a horizontal resolution of 1.8° (latitude) \times 3.6° (longitude) and 19 vertical levels, with 50 m vertical resolution near the surface. The marine ecosystem component has two phytoplankton (nitrogen fixers, regular phytoplankton) and one zooplankton groups. Detailed model set-up description and evaluation are in Yao et al. (2019, without iron configuration). Model results after a 3,000-year spin up are used in this study.

The GFDL-model combines the global climate model GFDL CM2.6 (Delworth et al., 2012) with the planktonic ecosystem model COBALT (Stock et al., 2014). Its ocean component has an approximate spatial resolution of 10 km and 50 vertical layers, with 10 m vertical resolution over the top 200 m. COBALT contains three phytoplankton (small, large, diazotrophs) and three zooplankton groups (micro-, meso-, macrozooplankton). Trophic interactions are size-based and designed to represent plankton physiology and predator-prey interactions (see Stock et al. (2017) for details). Model results after a 50-year simulation with fully coupled configuration, forced by year 1990 conditions, are used in this study.

The observationally based FCE is calculated following Stock and Dunne (2010) using satellite-based phytoplankton production estimates (VGPM; Behrenfeld & Falkowski, 1997). Mesozooplankton production is calculated using mesozooplankton biomass from the COPEPOD Database (O'Brien, 2007) and growth rate estimated following Hirst and Bunker (2003) based on temperature and chlorophyll from MODIS (<https://oceancolor.gsfc.nasa.gov/data/aqua/>). The seasonal pattern of the FCE is first normalized at each station and then averaged over a biome to avoid weighting large absolute values of the FCE higher. The seasonal cycles for specific locations with data coverage throughout the year yield similar results (Figure S5 in Supporting Information S1). The observed mixed layer depth (MLD) is taken from the ARGO mixed layer database (<http://mixedlayer.ucsd.edu/>) using the temperature threshold mean MLD (Holte et al., 2017), which was also used to infer the simulated MLD with a starting depth of 0.5–2 m. For detailed model MLD evaluations, please see Xue et al. (2022).

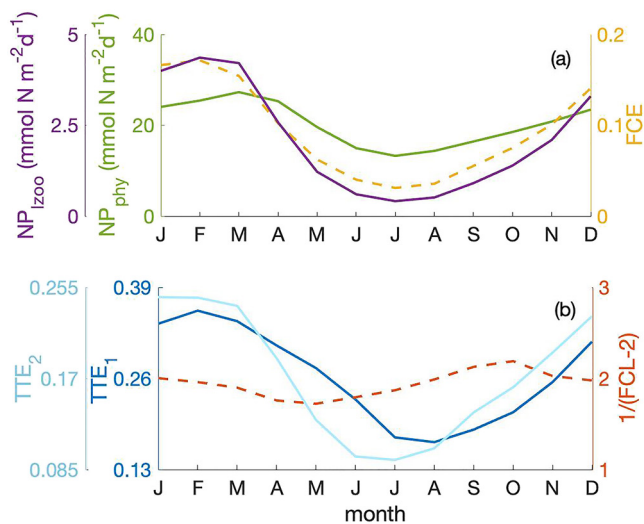


Figure 1. Trophic amplification due to seasonally varying trophic transfer efficiency (TTE): (a) Seasonal cycles of net phytoplankton (NP_{phy} , green), mesozooplankton production (NP_{izoo} , purple) and FCE (NP_{izoo}/NP_{phy} , yellow). The y axis range spans 100% of change relative to the annual mean for each variable; (b) seasonal cycles of the terms in Equation 8 to assess the relative contributions from trophic transfer efficiency between trophic levels 1 and 2 (TTE_1 , light blue) and trophic levels 2 and 3 (TTE_2 , dark blue), and food chain length (FCL; as $1/(FCL - 2)$, red) over the water column within the focus region. The y axis range spans 50% of change relative to the annual mean for each variable.

2.4. Biome Definition

The relation of MLD and FCE is analyzed globally, subdivided by productive and oligotrophic regions. Productive and oligotrophic regions are categorized by the annual mean surface chlorophyll above and below $0.1 \text{ mg Chl m}^{-3}$ for observational data and $0.15 \text{ mg Chl m}^{-3}$ for model results, respectively. A higher threshold for model simulations is used to account for the relatively high bias (Figure S2 in Supporting Information S1) and achieve similar biome distribution in comparison with observational estimates. Productive regions reflect the high-latitude, tropical and coastal regions with high macronutrient and pronounced phytoplankton concentrations. The oligotrophic regions generally correspond to the subtropical gyres.

3. Results and Discussion

3.1. Trophic Transfer Efficiency Drives Trophic Amplification

The amplitude of seasonal variations in mesozooplankton production is more prominent than that of phytoplankton, revealing the feature of trophic amplification on a seasonal scale (hereafter referred to as “seasonal trophic amplification,” Figure 1a). Phytoplankton and mesozooplankton production vary seasonally in phase, with high production in austral summer and low production in winter. The fraction of phytoplankton production resulting in mesozooplankton production, that is FCE, is 9.5% on average, which is roughly consistent with observational estimates (Figure S1 in Supporting Information S1), with a maximum of 17% in austral summer and a minimum of 3% in winter. The seasonal variation of the FCE is reflected in an amplified seasonal variation of mesozooplankton production (83% relative to its annual mean) compared to that of phytoplankton (35%).

Seasonal trophic amplification in our model is mainly introduced by variations in TTE, while FCL plays a negligible role (Figure 1b). As evident from Equation 8, variations of the FCE can be decomposed into effects from TTE and FCL. TTE varies seasonally in phase with net phytoplankton and mesozooplankton production, contributing most to the seasonal variation of the FCE and thus trophic amplification (Figure 1b). The seasonal variation of FCL is small by comparison. We, therefore, focus on TTE of seasonal trophic amplification in the following sections.

3.2. Taking a Mixed Layer Depth Perspective to Grazing

TTE, as the dominant driver of seasonal trophic amplification, is mainly affected by variations of predator grazing. The fate of phytoplankton production is either grazing by zooplankton, which is then used for respiration, egested as fecal pellets, or passed on to the next trophic level, or not to be consumed by grazers (Figures 2a and 2b). In austral winter, a relatively smaller fraction of phytoplankton production is being grazed (57%) than in summer (65%). The fraction of production that is passed on to the next trophic level (TTE) is also lower in winter (17%) than in summer (33%). The production of fecal pellets relative to phytoplankton production stays approximately the same in winter and summer (Figures 2a and 2b), while biomass-specific production of fecal pellets is substantially smaller in winter. While a larger share of phytoplankton production is used for zooplankton respiration in austral winter, this is due to reduced biomass-specific zooplankton grazing combined with a roughly constant biomass specific respiration rate (Figure 2c). Therefore, with reduced losses to fecal pellets in winter, and an approximately constant biomass-specific respiration, the dominant process determining how much production is available to the next trophic level, thus TTE, is predator grazing.

For predator grazing, predator-prey encounter efficiency, which is driven by the MLD, is more important than total (vertically integrated) prey biomass (Figure 3). If predator and prey are diluted over a deeper mixed layer, the potential for predator-prey encounters is smaller. We pick a month in austral summer and winter, respectively, that host roughly the same amount of vertically integrated prey biomass within the water column (60 mmol N m^{-2} ,

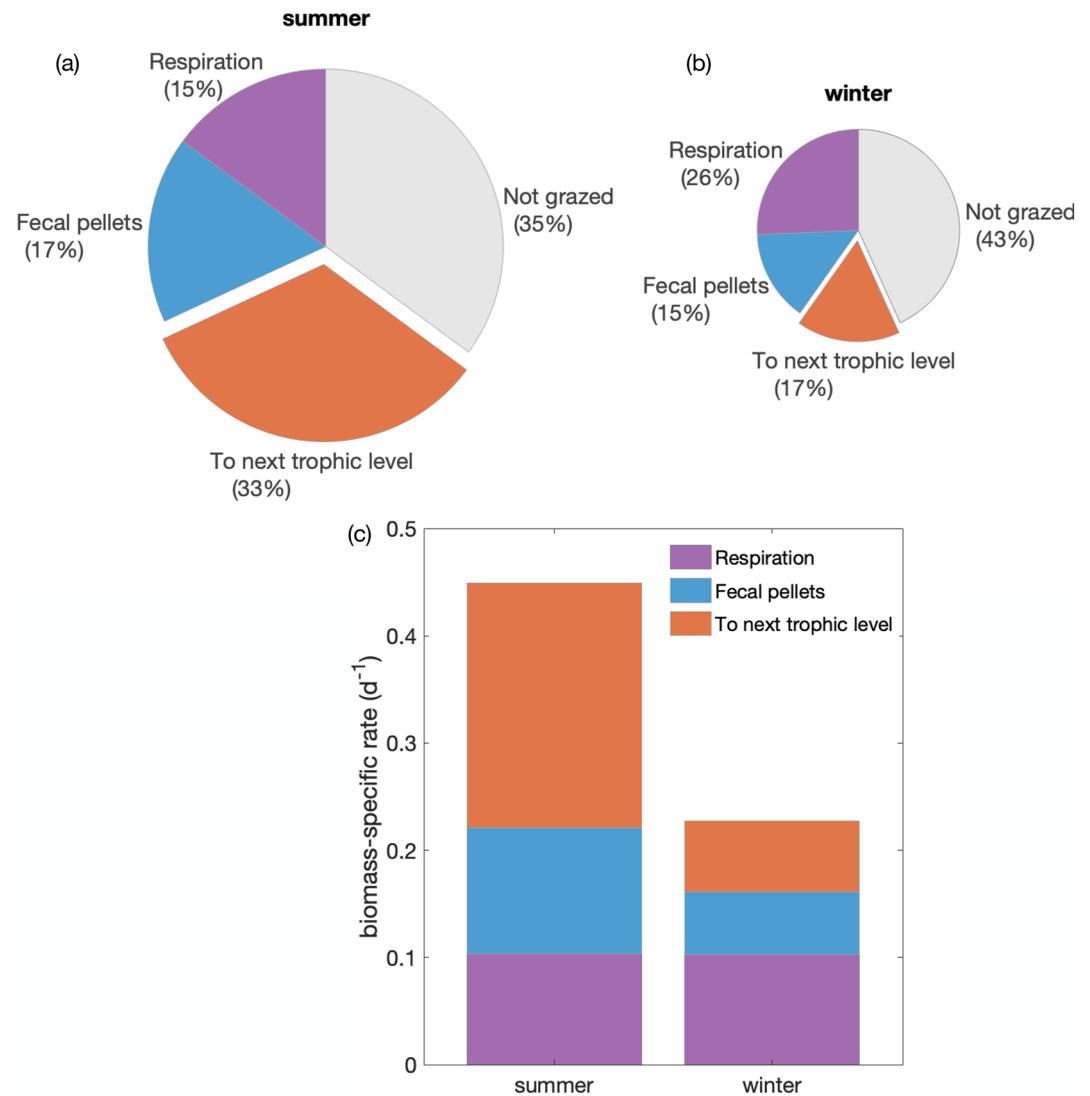


Figure 2. Reduced trophic transfer efficiency in winter (TTE) due to reduced efficiency of grazing: Fate of phytoplankton production in austral (a) summer; and (b) winter. The sizes of the pie charts are representative for the magnitude of phytoplankton production. (c) Biomass-specific rate of respiration (purple), fecal pellet production (blue) and production available to the next trophic level (red) in austral summer and winter. The sum of all colored components (respiration, fecal pellets and the production available to the next trophic level) represents zooplankton grazing; only the grazed (colored) parts are being processed by zooplankton.

Figure 3a) at different MLD (February: 10 m; June: 35 m). Predator and prey are more concentrated in a shallower mixed layer in February while they are more diluted in June. The high predator and prey concentration in a thinner layer allows the predator to graze more efficiently due to a high encounter efficiency, hence supporting a high specific grazing rate for the predator. This mechanism reflects a significant correlation between MLD and the vertical encounter efficiency (Figure 3b). Similar findings have also been proposed in a horizontal perspective that the spatial distribution drives the covariance of predator and prey and dominates over total biomass in regulating the system production and food web structure (e.g., front system; Benoit-Bird & McManus, 2012; Woodson & Litvin, 2015).

3.3. A Negligible Role of Food Web Structure?

Seasonal changes in food web structure, thus food chain length, have a negligible effect on the trophic amplification (Figure 1b). In our model, the food chain length varies very little around 2.5 (thus $1/(FCL - 2)$ stays

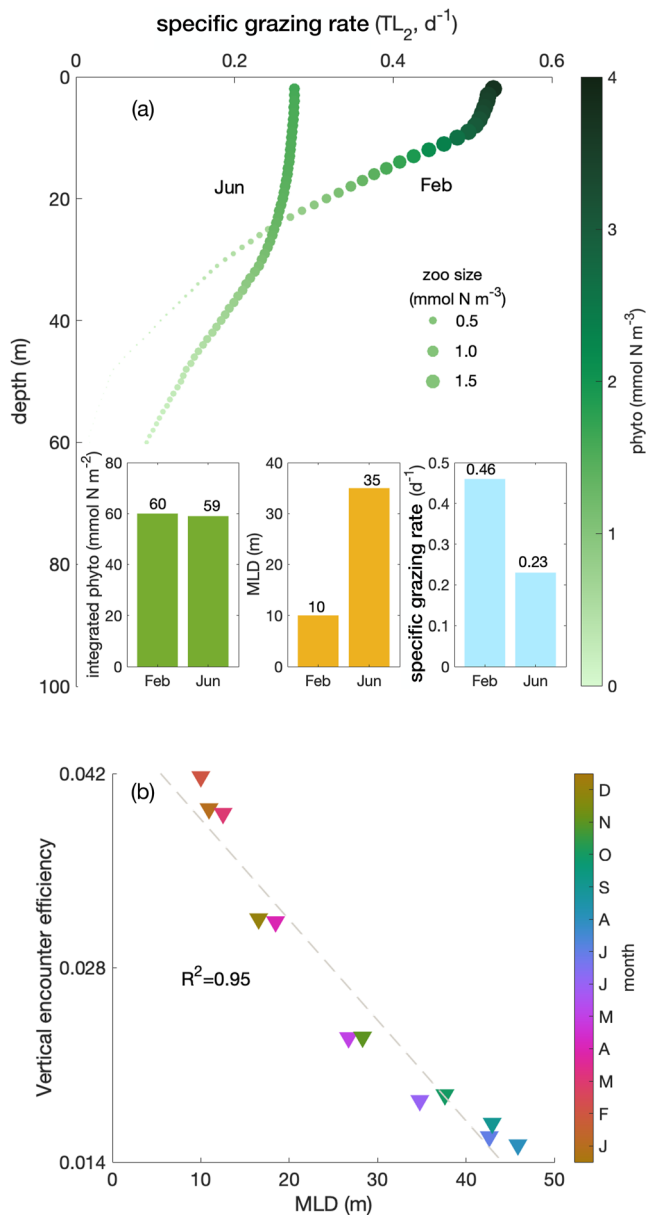


Figure 3. Reduced efficiency of grazing (specific grazing rate) due to prey dilution in deep winter mixed layers: (a) Vertical profiles of predator biomass specific grazing rate (d^{-1}) in February and June with color indicating the prey concentration (TL_1 , $mmol N m^{-3}$) and size of the circle indicating the predator concentration (TL_2 , $mmol N m^{-3}$) within the focus region; inserts show prey vertically integrated over the water column (green), the mixed layer depth (yellow), and the average mixed layer specific ingestion rate (light blue); (b) Correlation of mixed layer depth and vertical encounter efficiency (EE, Equation 9) with colors indicating the time of the year (months). R^2 value of the correlation is shown on the left side.

around 2), with mesozooplankton grazing nearly equally on phytoplankton and microzooplankton. The food chain tends to be shorter when the phytoplankton community is more strongly dominated by large phytoplankton, reflecting a more efficient food web structure.

The limited flexibility in our simulated food web structure, for example, through fixed diet preferences, cannot fully capture the complex trophic interactions of the real ecosystem. The predator diet preference in the model is fixed based on body size (Boyce et al., 2015), allowing only for a limited variation of the food web structure and FCL and their contribution to variations of the FCE. A previous study found that different FCL is the major cause of FCE differences across ocean biomes (Stock & Dunne, 2010). A deliberate change in food web structure (albeit limited to the lower trophic levels that the model resolves) by manipulating the diet of the two zooplankton groups does not have a notable effect in our model (see Supporting Information S1 for detailed sensitivity studies). But given the limitation of the simplified description of food web dynamics in the model, no general conclusions about the role of food web structure should be derived from this study.

3.4. MLD Driving Trophic Transfer: A Common Feature of Productive Regions

The negative correlation between MLD and FCE is not only apparent in the Humboldt system but also in other productive regions. To test the importance of the MLD for the FCE, we globally define “productive regions”, which include the Humboldt system, versus “oligotrophic regions” that are bottom-up limited and comparatively low in phytoplankton production (see Methods section). The spatial patterns of the simulated productive regions from the UVic-model and the GFDL-model generally match the observational estimates (Figures 4a–4c). A clear negative correlation of the FCE and the MLD in the productive regions (Figures 4d–4f) is apparent in the observational estimates and the model simulations. A relatively low FCE generally coincides with deep MLD, consistent with the dilution and concentration of prey reducing the predator-prey encounter efficiency, and thereby grazing and the FCE. Worth noticing, while the dominant mesozooplankton group in the Humboldt upwelling system has not been observed to do diel vertical migration (Massing et al., 2022), it has been commonly observed elsewhere. Despite using deep waters as a refuge during the day, diel vertical migration is unlikely to affect MLD and FCE correlations because zooplankton feed primarily near the surface (Hays, 2003), where prey is diluted regardless of zooplankton movement. Stock et al. (2014) compared annual average FCE across different regions of the globe and similarly found a comparatively prominent role of dilution of prey for the high latitude regions.

The seasonal variation of FCE is governed by different mechanisms in oligotrophic regions, with much lower correlation coefficients compared to productive regions (Figures 4g–4i). As oligotrophic regions are nutrient-limited, deepening mixed layers in the models bring up nutrients from below that stimulate phytoplankton growth. Mixing events have been observed in the North Pacific gyre to significantly increase not only phytoplankton production but also zooplankton biomass (McGowan & Hayward, 1978). When food availability for zooplankton is low, as is the case in oligotrophic regions, zooplankton growth efficiency is very sensitive to a given change in food. This is because the limited grazed food is needed to sustain basic functions (e.g., respiration), as zooplankton is “starving.” In contrast, zooplankton growth efficiency is much less sensitive to changes

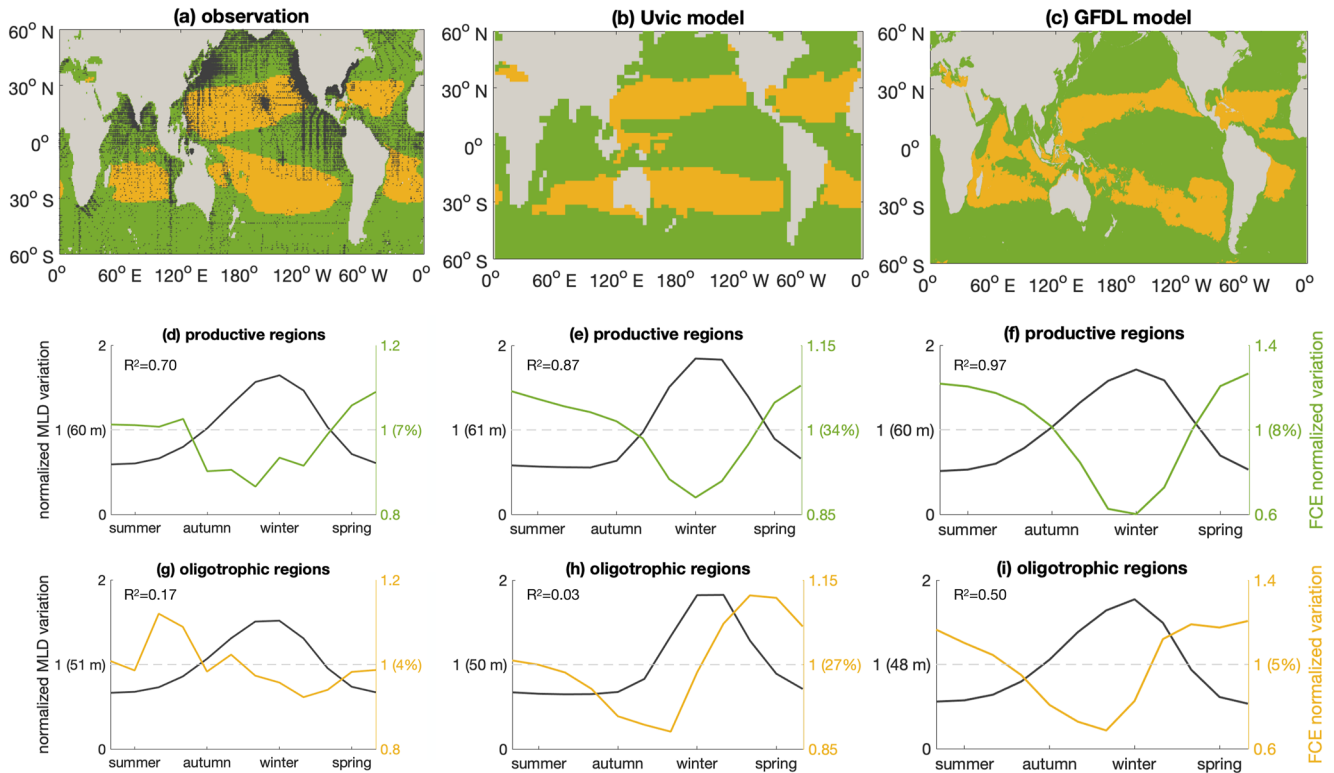


Figure 4. Indication for seasonal mixed layer depth (MLD) variations driving food chain efficiency (FCE) beyond the Humboldt system: Ocean biomes calculated from (a) observations, (b) UVic-model and (c) GFDL-model with productive (green, above $0.1 \text{ mg Chl m}^{-3}$ (observations)/ $0.15 \text{ mg Chl m}^{-3}$ (model)) and oligotrophic (yellow, below $0.1 \text{ mg Chl m}^{-3}$ (observations)/ $0.15 \text{ mg Chl m}^{-3}$ (model)) regions. Dots in (a) indicate the locations of observations. Average seasonal cycles of MLD (black) and food chain efficiency (FCE, the ratio of net mesozooplankton production to phytoplankton production, Equation 6, color) for (d and g) observations (e and h) UVic-model and (f and i) GFDL-model, normalized by the mean MLD and FCE for each biome: productive (green, (d to f) and oligotrophic (yellow, g to i) regions. Values in brackets indicate the absolute values of annual means. R^2 values of the correlations between MLD and FCE are shown in the top-left side of each panel.

in food concentration when food is plentiful (Figure 2 in Stock et al., 2014). Thus, in oligotrophic regions, one may expect a positive response of the FCE to deepening mixed layers, as partially indicated in the global models.

Both global models tend to capture the correlation between MLD and FCE in productive regions, regardless of different trophic resolutions. While the value of FCE in the GFDL-model roughly matches the observed estimate of 6% in the productive regions, the value of FCE is much higher in the UVic-model, possibly due to resolving only one trophic link. Nevertheless, in agreement with the classic paradigm (Ryther, 1969), the FCE in both models is generally higher in productive than in oligotrophic regions.

4. Implications and Conclusions

Our model simulates seasonal trophic amplification driven by mixed layer dynamics in the Humboldt and other productive systems. To pinpoint the origin of the seasonal amplification, we have applied an analytical approach that allowed us to define and disentangle the contributions to the seasonal variation of the food chain efficiency (FCE) of the efficiency of production transfer between trophic levels (TTE), and the length of the food chain up to the top predator (FCL). In our model, the TTE is the main contributor to the seasonal amplification in the Humboldt system, and it is mainly driven by the mixed layer dynamics. The same mechanism also seems to apply to other oceanic biomes characterized by elevated chlorophyll, such as coastal and high latitude oceans. A caveat of our models is that the food web structures do not fully resolve the complexity of the real ecosystem, that is, seasonal variations of the FCL may play a larger role in the real ocean. Our results highlight that the annual values of FCE typically analyzed by previous studies emerge from a dynamic seasonal cycle.

The term trophic amplification was coined in analyses of climate change projections, with ocean warming affecting more strongly the higher than the lower trophic levels (Chust et al., 2014; Kirby & Beaugrand, 2009;

Kwiatkowski et al., 2019; Lotze et al., 2019; Stock et al., 2014). Different responses of phytoplankton biomass are projected by climate models for low versus high latitude regions with global warming. Positive trophic amplification, with increases of biomass in each trophic level, is found more commonly in high latitude regions. Stock et al. (2014) suggest that shoaling of winter mixed layers and ice melting due to global warming may play a role, leading to productivity increases and tighter coupling between predators and prey. In contrast, increased nutrient limitation arising from enhanced stratification may cause negative trophic amplification in low latitude regions (Chust et al., 2014; Kwiatkowski et al., 2019; Stock et al., 2014).

We note that next to mixed layer dynamics other mechanisms may affect predator-prey encounters, with the potential to further intensify trophic amplification, such as expanding oxygen minimum zones. Schukat et al. (2021) observed in the Humboldt system that key mesozooplankton species, such as calanoid copepods, almost exclusively restrict themselves to the surface layer above the oxygen minimum zone, allowing the Peruvian anchovies to forage more easily and efficiently and supporting the high fish yield in the Humboldt system. We hypothesize a potential positive feedback loop where positive amplification triggered by shallowing mixed layers, or a shoaling of the oxycline, increases the export of organic material to the deeper ocean, as a result of both enhanced phytoplankton production and export efficiency (Xue et al., 2022). The enhanced export then could lead to enhanced oxygen consumption at depth, and to a further expansion of the oxygen minimum zone (Riebesell et al., 2007), resulting in further enhanced prey concentration and trophic amplification, and in turn more export, thereby closing the feedback loop.

Based on our findings of the present-day seasonality of the Humboldt lower trophic ecosystem dynamics, we suggest that positive trophic amplification may promote export of organic material under global warming not only in the Humboldt system but also in the high latitudes as a result of both increasing phytoplankton production (e.g., Sallée et al., 2013, 2021), and higher food chain efficiency (Chust et al., 2014; Kwiatkowski et al., 2019; Stock et al., 2014) with shallowing mixed layers. Improving understanding of seasonal dynamics may facilitate the interpretation of ecosystem sensitivities in observational data, and help to further improve the simulation of sensitivities in climate models, thereby improving climate projections.

Data Availability Statement

Regional model (CROCO-BioEBUS) data is available through Xue et al. (2022). Global model data is available through Yao et al. (2019) for the UVic model data and Stock et al. (2017) for the GFDL model data.

Acknowledgments

The authors thank two anonymous reviewers for their constructive comments. This work is financially supported by the China Scholarship Council (TX, grant no. 201808460055) and the BMBF funded projects Coastal Upwelling System in a Changing Ocean (CUSCO; IF and AO, Grant No. 03F0813A) and Humboldt Tipping (HTP; IF and AO, grant no. 01LC1823B). The authors would like to thank Jessica Luo for constructive feedback and Wanxuan Yao for providing the UVic model data. Open Access funding enabled and organized by Projekt DEAL.

References

- Bakun, A., & Weeks, S. J. (2008). The marine ecosystem off Peru: What are the secrets of its fishery productivity and what might its future hold? *Progress in Oceanography*, 79(2–4), 290–299. <https://doi.org/10.1016/j.pocean.2008.10.027>
- Behrenfeld, M. J., & Falkowski, P. G. (1997). Photosynthetic rates derived from satellite-based chlorophyll concentration. *Limnology & Oceanography*, 42(1), 1–20. <https://doi.org/10.4319/llo.1997.42.1.0001>
- Benoit-Bird, K. J., & McManus, M. A. (2012). Bottom-up regulation of a pelagic community through spatial aggregations. *Biology Letters*, 8(5), 813–816. <https://doi.org/10.1098/rsbl.2012.0232>
- Bertrand, A., Segura, M., Gutiérrez, M., & Vásquez, L. (2004). From small-scale habitat loopholes to decadal cycles: A habitat-based hypothesis explaining fluctuation in pelagic fish populations off Peru. *Fish and Fisheries*, 5(4), 296–316. <https://doi.org/10.1111/j.1467-2679.2004.00165.x>
- Boyce, D. G., Frank, K. T., & Leggett, W. C. (2015). From mice to elephants: Overturning the ‘one size fits all’ paradigm in marine plankton food chains. *Ecology Letters*, 18(6), 504–515. <https://doi.org/10.1111/ele.12434>
- Carton, J. A., & Giese, B. S. (2008). A reanalysis of ocean climate using Simple Ocean Data Assimilation (SODA). *Monthly Weather Review*, 136(8), 2999–3017. <https://doi.org/10.1175/2007MWR1978.1>
- Chavez, F. P., Bertrand, A., Guevara-Carrasco, R., Soler, P., & Csirke, J. (2008). The northern Humboldt Current System: Brief history, present status and a view towards the future. *Progress in Oceanography*, 79(2–4), 95–105. <https://doi.org/10.1016/j.pocean.2008.10.012>
- Chust, G., Allen, J. I., Bopp, L., Schrum, C., Holt, J., Tsiaras, K., et al. (2014). Biomass changes and trophic amplification of plankton in a warmer ocean. *Global Change Biology*, 20(7), 2124–2139. <https://doi.org/10.1111/gcb.12562>
- Delworth, T. L., Rosati, A., Anderson, W., Adcroft, A. J., Balaji, V., Benson, R., et al. (2012). Simulated climate and climate change in the GFDL CM2.5 high-resolution coupled climate model. *Journal of Climate*, 25(8), 2755–2781. <https://doi.org/10.1175/JCLI-D-11-00316.1>
- Dickman, E. M., Newell, J. M., González, M. J., & Vanni, M. J. (2008). Light, nutrients, and food-chain length constrain planktonic energy transfer efficiency across multiple trophic levels. *Proceedings of the National Academy of Sciences*, 105(47), 18408–18412. <https://doi.org/10.1073/pnas.0805566105>
- Du Pontavice, H., Gascuel, D., Reygondeau, G., Maureaud, A., & Cheung, W. W. (2020). Climate change undermines the global functioning of marine food webs. *Global Change Biology*, 26(3), 1306–1318. <https://doi.org/10.1111/gcb.14944>
- Echevin, V., Aumont, O., Ledesma, J., & Flores, G. (2008). The seasonal cycle of surface chlorophyll in the Peruvian upwelling system: A modelling study. *Progress in Oceanography*, 79(2–4), 167–176. <https://doi.org/10.1016/j.pocean.2008.10.026>
- Friedland, K. D., Stock, C., Drinkwater, K. F., Link, J. S., Leaf, R. T., Shank, B. V., et al. (2012). Pathways between primary production and fisheries yields of large marine ecosystems. *PLoS One*, 7(1), e28945. <https://doi.org/10.1371/journal.pone.0028945>

- Gutknecht, E., Dadou, I., Le Vu, B., Cambon, G., Sudre, J., Garçon, V., et al. (2013). Coupled physical/biogeochemical modeling including O₂-dependent processes in the eastern boundary upwelling systems: Application in the Benguela. *Biogeosciences*, 10(6), 3559–3591. <https://doi.org/10.5194/bg-10-3559-2013>
- Hays, G. C. (2003). A review of the adaptive significance and ecosystem consequences of zooplankton diel vertical migrations. *Migrations and Dispersal of Marine Organisms*, 163–170. https://doi.org/10.1007/978-94-017-2276-6_18
- Heneghan, R. F., Everett, J. D., Blanchard, J. L., & Richardson, A. J. (2016). Zooplankton are not fish: Improving zooplankton realism in size-spectrum models mediates energy transfer in food webs. *Frontiers in Marine Science*, 3, 201. <https://doi.org/10.3389/fmars.2016.00201>
- Hirst, A., & Bunker, A. (2003). Growth of marine planktonic copepods: Global rates and patterns in relation to chlorophyll a, temperature, and body weight. *Limnology & Oceanography*, 48(5), 1988–2010. <https://doi.org/10.4319/lo.2003.48.5.1988>
- Holte, J., Talley, L. D., Gilson, J., & Roemmich, D. (2017). An Argo mixed layer climatology and database. *Geophysical Research Letters*, 44(11), 5618–5626. <https://doi.org/10.1002/2017GL073426>
- Keller, D., Oschlies, A., & Eby, M. (2012). A new marine ecosystem model for the University of Victoria Earth System Climate Model. *Geoscientific Model Development*, 5(5), 1195–1220. <https://doi.org/10.5194/gmd-5-1195-2012>
- Kirby, R. R., & Beaugrand, G. (2009). Trophic amplification of climate warming. *Proceedings of the Royal Society B: Biological Sciences*, 276(1676), 4095–4103. <https://doi.org/10.1098/rspb.2009.1320>
- Kwiatkowski, L., Aumont, O., & Bopp, L. (2019). Consistent trophic amplification of marine biomass declines under climate change. *Global Change Biology*, 25(1), 218–229. <https://doi.org/10.1111/gcb.14468>
- Legendre, L., & Rassoulzadegan, F. (1996). Food-web mediated export of biogenic carbon in oceans: Hydrodynamic control. *Marine Ecology Progress Series*, 145, 179–193. <https://doi.org/10.3354/meps145179>
- Lindeman, R. L. (1942). The trophic-dynamic aspect of ecology. *Ecology*, 23(4), 399–417. <https://doi.org/10.2307/1930126>
- Lotze, H. K., Tittensor, D. P., Bryndum-Buchholz, A., Eddy, T. D., Cheung, W. W., Galbraith, E. D., et al. (2019). Global ensemble projections reveal trophic amplification of ocean biomass declines with climate change. *Proceedings of the National Academy of Sciences*, 116(26), 12907–12912. <https://doi.org/10.1073/pnas.1900194116>
- Massing, J. C., Schukat, A., Auel, H., Auch, D., Kittu, L., Pinedo Arteaga, E. L., et al. (2022). Toward a solution of the “Peruvian puzzle”: Pelagic food-web structure and trophic interactions in the northern Humboldt current upwelling system off Peru. *Frontiers in Marine Science*, 8. Art–Nr. <https://doi.org/10.3389/fmars.2021.759603>
- McGowan, J. A., & Hayward, T. L. (1978). Mixing and oceanic productivity. *Deep-Sea Research*, 25(9), 771–793. [https://doi.org/10.1016/0146-6291\(78\)90023-1](https://doi.org/10.1016/0146-6291(78)90023-1)
- Mitra, A., Castellani, C., Gentleman, W. C., Jónasdóttir, S. H., Flynn, K. J., Bode, A., et al. (2014). Bridging the gap between marine biogeochemical and fisheries sciences; configuring the zooplankton link. *Progress in Oceanography*, 129, 176–199. <https://doi.org/10.1016/j.pocean.2014.04.025>
- O’Brien, T. D. (2007). COPEPOD, a global plankton database: A review of the 2007 database contents and new quality control methodology. O’Reilly, J. E., Maritorena, S., Mitchell, B. G., Siegel, D. A., Carder, K. L., Garver, S. A., et al. (1998). Ocean color chlorophyll algorithms for SeaWiFS. *Journal of Geophysical Research*, 103(C11), 24937–24953. <https://doi.org/10.1029/98JC02160>
- Pauly, D., & Christensen, V. (1995). Primary production required to sustain global fisheries. *Nature*, 374(6519), 255–257. <https://doi.org/10.1038/374255a0>
- Prowe, A. F., Visser, A. W., Andersen, K. H., Chiba, S., & Kiørboe, T. (2019). Biogeography of zooplankton feeding strategy. *Limnology & Oceanography*, 64(2), 661–678. <https://doi.org/10.1002/lno.11067>
- Ridgway, K., Dunn, J., & Wilkin, J. (2002). Ocean interpolation by four-dimensional weighted least squares—Application to the waters around Australasia. *Journal of Atmospheric and Oceanic Technology*, 19(9), 1357–1375. [https://doi.org/10.1175/1520-0426\(2002\)019%3C1357:OIBFDW%3E2.0.CO;2](https://doi.org/10.1175/1520-0426(2002)019%3C1357:OIBFDW%3E2.0.CO;2)
- Riebesell, U., Schulz, K. G., Bellerby, R., Botros, M., Fritsche, P., Meyerhöfer, M., et al. (2007). Enhanced biological carbon consumption in a high CO₂ ocean. *Nature*, 450(7169), 545–548. <https://doi.org/10.1038/nature06267>
- Ryther, J. H. (1969). Photosynthesis and fish production in the sea. *Science*, 166(3901), 72–76. <https://doi.org/10.1126/science.166.3901.72>
- Sallée, J.-B., Pellichero, V., Akhondas, C., Pauthenet, E., Vignes, L., Schmidtko, S., et al. (2021). Summertime increases in upper-ocean stratification and mixed-layer depth. *Nature*, 591(7851), 592–598. <https://doi.org/10.1038/s41586-021-03303-x>
- Sallée, J.-B., Shuckburgh, E., Bruneau, N., Meijers, A. J., Bracegirdle, T. J., & Wang, Z. (2013). Assessment of Southern Ocean mixed-layer depths in CMIP5 models: Historical bias and forcing response. *Journal of Geophysical Research: Oceans*, 118(4), 1845–1862. <https://doi.org/10.1002/jgrc.20157>
- Schukat, A., Hagen, W., Dorschner, S., Acosta, J. C., Arteaga, E. L. P., Ayón, P., & Auel, H. (2021). Zooplankton ecological traits maximize the trophic transfer efficiency of the Humboldt Current upwelling system. *Progress in Oceanography*, 193, 102551. <https://doi.org/10.1016/j.pocean.2021.102551>
- Shchepetkin, A. F., & McWilliams, J. C. (2005). The regional oceanic modeling system (ROMS): A split-explicit, free-surface, topography-following-coordinate oceanic model. *Ocean Modelling*, 9(4), 347–404. <https://doi.org/10.1016/j.ocemod.2004.08.002>
- Stock, C., & Dunne, J. (2010). Controls on the ratio of mesozooplankton production to primary production in marine ecosystems. *Deep Sea Research Part I: Oceanographic Research Papers*, 57(1), 95–112. <https://doi.org/10.1016/j.dsr.2009.10.006>
- Stock, C., Dunne, J., & John, J. (2014). Drivers of trophic amplification of ocean productivity trends in a changing climate. *Biogeosciences*, 11(24), 7125–7135. <https://doi.org/10.5194/bg-11-7125-2014>
- Stock, C., Dunne, J. P., & John, J. G. (2014). Global-scale carbon and energy flows through the marine planktonic food web: An analysis with a coupled physical–biological model. *Progress in Oceanography*, 120, 1–28. <https://doi.org/10.1016/j.pocean.2013.07.001>
- Stock, C., John, J. G., Rykaczewski, R. R., Asch, R. G., Cheung, W. W., Dunne, J. P., et al. (2017). Reconciling fisheries catch and ocean productivity. *Proceedings of the National Academy of Sciences*, 114(8), E1441–E1449. <https://doi.org/10.1073/pnas.1610238114>
- Ulanowicz, R. E. (1995). *Ecosystem trophic foundations: Lindeman exonerata. Complex ecology: The part-whole relation in ecosystems* (pp. 549–550). Prentice Hall.
- Weaver, A. J., Eby, M., Wiebe, E. C., Bitz, C. M., Duffy, P. B., Ewen, T. L., et al. (2001). The UVic Earth System Climate Model: Model description, climatology, and applications to past, present and future climates. *Atmosphere-Ocean*, 39(4), 361–428. <https://doi.org/10.1080/07055900.2001.9649686>
- Woodson, C. B., & Litvin, S. Y. (2015). Ocean fronts drive marine fishery production and biogeochemical cycling. *Proceedings of the National Academy of Sciences*, 112(6), 1710–1715. <https://doi.org/10.1073/pnas.1417143112>
- Worley, S. J., Woodruff, S. D., Reynolds, R. W., Lubker, S. J., & Lott, N. (2005). ICOADS release 2.1 data and products. *International Journal of Climatology: A Journal of the Royal Meteorological Society*, 25(7), 823–842. <https://doi.org/10.1002/joc.1166>

- Xue, T., Frenger, I., Prowe, A., José, Y. S., & Oschlies, A. (2022). Mixed layer depth dominates over upwelling in regulating the seasonality of ecosystem functioning in the Peruvian Upwelling System. *Biogeosciences*, *19*(2), 455–475. <https://doi.org/10.5194/bg-19-455-2022>
- Yao, W., Kvale, K. F., Achterberg, E., Koeve, W., & Oschlies, A. (2019). Hierarchy of calibrated global models reveals improved distributions and fluxes of biogeochemical tracers in models with explicit representation of iron. *Environmental Research Letters*, *14*(11), 114009. <https://doi.org/10.1088/1748-9326/ab4c52>

References From the Supporting Information

- D'Alelio, D., Libralato, S., Wyatt, T., & d'Alcalà, M. R. (2016). Ecological-network models link diversity, structure and function in the plankton food-web. *Scientific Reports*, *6*(1), 1–13. <https://doi.org/10.1038/srep21806>